

An explanation for experimental behavior of hybrid metallocene silica-supported catalyst for ethylene polymerization

Sílvia Rodrigues^a, Fernando Silveira^a, J.H.Z. dos Santos^a, M.L. Ferreira^{b,*}

^a Instituto de Química da UFRGS, Av. Bento Gonçalves 9500, 91501-970 Porto Alegre, Brazil

^b PLAPIQUI-UNS-CONICET, Camino La Carrindanga Km 7, CC 717 8000 Bahía Blanca, Argentina

Received 24 December 2003; received in revised form 21 January 2004; accepted 4 February 2004

Available online 12 March 2004

Abstract

This work presents the results of homopolymerization of ethylene using an hybrid system $(n\text{BuCp})_2\text{ZrCl}_2\text{-Cp}_2\text{ZrCl}_2$, supported on silica. The catalytic systems were analyzed by RBS, DRIFTS and EXAFS and polyethylenes (PE) by GPC and DSC. The catalytic activities and the polymer properties showed dependence on the different ratio used $(n\text{BuCp})_2\text{ZrCl}_2/\text{Cp}_2\text{ZrCl}_2$ at the preparation step. Theoretical studies permit us to conclude that the metallocenes interact with the surface in different ways. Depending on the addition order and the molar ratio between both metallocenes, distribution and nature of active species would be different. Possibility of binuclear active sites with different propagation and termination constants is analyzed and discussed. EHMO calculations allow us to conclude that Cp_2ZrCl_2 has a strong affinity by AIS plane, whereas $(n\text{BuCp})_2\text{ZrCl}_2$ shows similar affinity for both silica planes.

© 2004 Elsevier B.V. All rights reserved.

Keywords: Supported metallocenes; Zirconocene; Theoretical characterization

1. Introduction

Metallocene/methylaluminoxane (MAO) systems combine high activity in α -olefins polymerization with the possibility of tailoring polymer properties, such as molecular weight (Mw) and molecular weight distribution (MwD) as well as stereochemical structure through a suitable ligand design around the metal center. However, such catalyst systems should be modified in order to be employed in the existent industrial plants. These modifications basically imply their immobilization onto supports, mainly on silica [1,2]. The use of the supported system improves the morphologic control of the resulting polymers, increases polymer bulk density, and may reduce the use of MAO [3].

In polymer processing, the molecular weight and the molecular weight distribution are important factors since they determine both the mechanical and the rheological properties, respectively. Metallocene are characterised by producing polymers with narrow molecular weight and composition distributions, which lead to many improvements in physical properties, such as clarity, impact resistance,

and environmental crack resistance. On the other hand, PE with a broad MwD show greater flowability in the molten state at high shear rate, which is important for blowing and extrusion techniques.

Thus industrial application of metallocene-based processes is restrained by two factors, the necessity to heterogeneize them and to produce polymers with broader MwD. One approach to achieve these goals resides in the immobilization of two different catalyst systems on the same support. Few examples have dealt with this approach. Kim et al. studied hybrid metallocene systems based on Zr and Hf derivatives. By varying the H_2 concentration in the reaction, the authors obtained polymers showing bimodality [4]. D'Agnillo et al. [5] reported the production of bimodal polymers employing hybrid systems— $\text{Et}(\text{Ind})_2\text{ZrCl}_2/\text{Cp}_2\text{TiCl}_2$. Han et al. tested two hybrid metallocene systems using MAO as co-catalyst: $\text{Cp}_2\text{TiCl}_2/\text{Cp}_2\text{ZrCl}_2$ and $\text{Cp}_2\text{ZrCl}_2/\text{Et}(\text{Ind})_2\text{ZrCl}_2$ [6]. The former produced bimodal polymer ($\text{Mw}/\text{Mn} = 3.5$). Nevertheless, in the the latter, each catalyst produces polymers with similar Mw values and therefore no bimodality was observed ($\text{Mw}/\text{Mn} = 4.0$), except varying the temperature during the polymerization, which might have influenced in the propagation ratio and termination reactions.

* Corresponding author. Tel.: +54-2914861700; fax: +54-2914861600.
E-mail address: mlferreira@plapiqui.edu.ar (M.L. Ferreira).

The combination of Ziegler-Natta and metallocene was also reported in the literature. A hybrid catalyst was generated by the immobilization of a Ziegler-Natta catalyst and Cp_2ZrCl_2 onto a support $\text{MgCl}_2/\text{SiO}_2$ which was prepared by the sol-gel technique. The resulting polymers showed high polydispersity (M_w/M_n between 3.5 and 95) [7–9]. Modification of a commercial Ziegler-Natta catalyst with CpTiCl_3 afforded two different species [10].

In previous works, we evaluated the effect of grafting $(n\text{BuCp})_2\text{ZrCl}_2$ and Cp_2ZrCl_2 onto silica under different molar ratio and addition sequence on the resulting metal content, on the catalyst activity and on polymer properties [11,12]. Theoretical and experimental previous works on $(n\text{BuCp})_2\text{ZrCl}_2/\text{SiO}_2$ allowed us to discuss experimental data considering the structure and interaction of zirconocenes with the support [13,14]. In the present work, a theoretical work of the nature of the surface species generated by grafting both $(n\text{BuCp})_2\text{ZrCl}_2$ and Cp_2ZrCl_2 onto silica is proposed.

2. Experimental and methods

2.1. Materials

All the chemicals were manipulated under inert atmosphere using the Schlenk technique. Silica Grace 956 ($200\text{ m}^2\text{ g}^{-1}$) was activated under vacuum ($P < 10^{-5}$ mbar) for 15 h at 450°C . $(n\text{BuCp})_2\text{ZrCl}_2$ and Cp_2ZrCl_2 (Aldrich) were used without further purification. Pure argon (White Martins) was passed through molecular sieves columns. MAO (gently supplied by Witco, 10.0 wt.% toluene solution, average molar mass 900 g mol^{-1}). Pure ethylene and argon (White Martins) were used. Pure grade toluene were deoxygenated and dried by standard techniques before use.

2.2. Preparation of supported catalysts

In a typical catalyst preparation, 1:3 Cp: $n\text{Bu}$ system was prepared by adding a Cp_2ZrCl_2 toluene solution to 1.0 g of activated silica corresponding to 0.25 wt.% Zr/ SiO_2 and stirred at room temperature for 30 min. After removing the solvent, a $(n\text{BuCp})_2\text{ZrCl}_2$ toluene solution corresponding to 0.75 wt.% Zr/ SiO_2 was added and the resulting slurry was stirred for 30 min at room temperature, and then filtered through a fritted disk. The resulting solid was washed with $15 \times 2.0\text{ cm}^3$ of toluene and dried under vacuum for 4 h. More experimental details are reported elsewhere [11]. In all preparation, initial Zr nominal total percentage was 1.0 wt.% Zr/ SiO_2 .

2.3. Characterization of supported catalysts

2.3.1. Rutherford backscattering spectrometry (RBS)

Zirconium loadings in catalysts were determined by RBS using He^+ beams of 2.0 MeV incidents on homogeneous

tablets of the compressed (12 MPa) powder of the catalyst systems. During analysis the base pressure in the chamber is kept in the 10^{-7} mbar range using membrane (to prevent oil contamination of the sample) and turbodrag molecular pump. The method is based on the determination of the number and the energy of the detected particles which are elastically scattered in the Coulombic field of the atomic nuclei in the target. In this study, the Zr/Si atomic ratio was determined from the heights of the signals corresponding to each of the elements in the spectra and converted to wt.% Zr/ SiO_2 . For an introduction to the method and applications of this technique the reader is referred elsewhere [15,16].

2.3.2. X-ray absorption fine structure (EXAFS) spectroscopy

X-ray absorption spectra were recorded on the Synchrotron Radiation Source at the Laboratório Nacional de Luz Sincrotron (Campinas). Measurements at the Zr K edge were performed at the LNLS XAS beam line using a Si (220) monochromator. The standard compounds were measured in transmission mode using two ion chambers filled with Ar. The samples of the catalysts were measured in fluorescence mode using an ion chamber and a NaI scintillator. Pellets were prepared from the catalysts powders in a globebox and covered with Kapton tape to avoid any oxidation by the air exposure. The measurements were carried out with the sample at room temperature.

The EXAFS analysis was performed using the WINXAS program [17]. The phase shift and amplitudes were obtained from the FEFF code [18].

2.3.3. Diffuse reflectance infrared spectroscopy (DRIFTS)

The solid catalysts were analyzed as powder in a DRIFT accessory, equipped with sampling cup. The spectra were recorded at room temperature on a Bomem MB-102 Spectrometer, coadding 36 scan at resolution of 4 cm^{-1} . This study was restricted to the mid-IR region ($4000\text{--}1100\text{ cm}^{-1}$) due to strong bulk absorption of silica in low wavenumber region. The spectra were collected as reflectance units and transformed to Kubelka-Munk (KM) units. All the measurements were performed at nitrogen atmosphere.

2.4. Polymerization reactions

Polymerizations were performed in 0.30 dm^3 of toluene in a 1.00 dm^3 Pyrex glass reactor connected to a constant temperature circulator and equipped with mechanical stirring and inlets for argon and the monomers. For each experiment, a mass of catalyst system corresponding to $10^{-5}\text{ mol l}^{-1}$ of Zr was suspended in 0.01 dm^3 of toluene and transferred into the reactor under argon. The polymerizations were performed at atmospheric pressure of ethylene at 60°C for 30 min at $\text{Al/Zr} = 1000$, using MAO as cocatalyst. Acidified (HCl) ethanol was used to quench the processes, and reaction products were separated by filtration, washed with distilled water, and finally dried under reduced pressure at 60°C .

2.5. Polyethylene characterization

Molar masses and molar mass distributions were investigated with a Waters CV plus 150 °C high-temperature GPC instrument, equipped with viscosimetric detector, and three Styragel HT type columns (HT3, HT4 and HT6) with exclusion limit 1×10^7 for polystyrene. 1,2,4-trichlorobenzene was used as solvent, at a flow rate of $1 \text{ cm}^3 \text{ min}^{-1}$. The analyses were performed at 140 °C. The columns were calibrated with standard narrow molar mass distribution polystyrenes and with linear low density polyethylenes and polypropylenes.

Polymer melting points (T_m) and crystallinities (χ_c) were determined on a Polymer Laboratories DSC differential scanning calorimeter calibrated with Indium, using a heating rate of 20 °C min^{-1} in the temperature range 30–150 °C. The heating cycle was performed twice, but only the results of the second scan are reported, because the former is influenced by the mechanical and thermal history of the samples.

2.6. The theoretical method

The molecular orbital calculations were carried out by means of an Extended Huckel modified method (EHMO). This semiempirical procedure provides a useful preliminary approach and has been used to study electronic changes in adsorption reactions and is useful for obtaining qualitative trends in adsorption processes [19]. In this method, the non-diagonal elements of one electron Extended Hückel Hamiltonian are proportional to the overlap matrix elements [20].

The program used was ICONC, which was developed by Calzaferri and co-workers [21] and includes repulsive terms to the total energy, which are not explicitly included in the EHMO. The repulsive coulombic energy is taken into account in a pairwise term. The total energy (E_t) of our adsorbate/substrate system is expressed as:

$$E_t = \sum n_i E_i + \frac{1}{2} \sum_i \sum_{i \neq j} E_{\text{rep}(i,j)}$$

The first term in the preceding expression corresponds to the attractive valence electron contribution (n_i) and the second term to the pairwise interatomic repulsions. Each valence level i has an associated energy E_i with occupancy n_i . The repulsion energy of a nucleus i in the presence of a fixed atom j is calculated as an electrostatic term and the summation extended to all possible atom pairs (E_{rep}).

2.6.1. The SiO₂ surface

The surface of amorphous silica can be considered from the structure of β -cristobalite [22]. There are two main planes: (100) and (111). The (111) plane or AIS contains isolated silanols (Si–OH), whereas at the (100) plane or GEM geminal groups are located Si(OH)₂. The (111) plane was modelled with 115 atoms, whereas the (100)

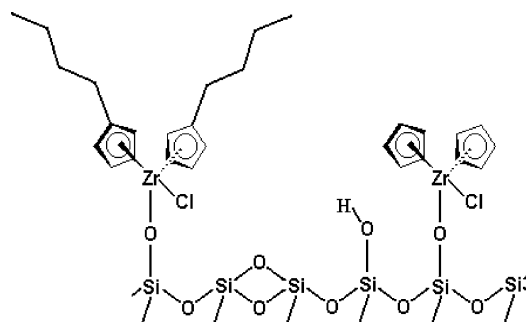


Fig. 1. Surface species of $(n\text{BuCp})_2\text{ZrCl}_2$ and Cp_2ZrCl_2 onto SiO_2AIS .

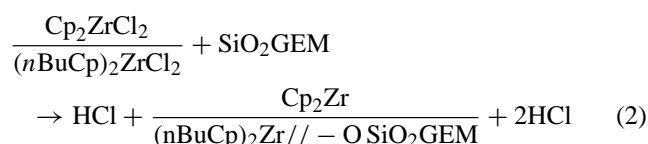
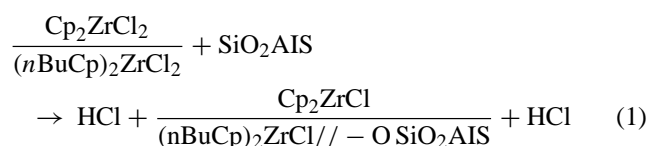
plane was modelled with 58 atoms. These OH groups have enough Brönsted acidity to react with zirconocenes, such as $(n\text{BuCp})_2\text{ZrCl}_2$ and Cp_2ZrCl_2 generating supported species and liberating HCl. Fig. 1 represents the surface species for both zirconocenes on the SiO_2 AIS plane. The real amorphous structure looks 85% like (111) plane. Since the real structure has defects and grain borders which are very difficult to model we think that following this approach in our model is nearer to the real situation for the surface and its adsorption capabilities [14].

2.6.2. The zirconocenes

The zirconocenes were modelled with all their atoms, considering the structural information available [23–25]. The structures of $(n\text{BuCp})_2\text{ZrCl}_2$ and Cp_2ZrCl_2 grafted on silica are represented in Fig. 1.

2.6.3. The surface reactions

To understand the interaction between the zirconocenes with SiO_2 structure at the molecular level and to correlate it with the supported species, a theoretical calculation was done. The reactions to be considered are:



The active sites are considered to be located on SiO_2AIS because SiO_2GEM produces inactive zirconium sites.

3. Results and discussion

In the following discuss along the text we will report Cp_2ZrCl_2 and $(n\text{BuCp})_2\text{ZrCl}_2$ for as Cp and $n\text{Bu}$, respectively. Besides, for the supported systems, the employed abbreviations report the addition order and the molar ratio.

Table 1
Zr content for different catalysts [11]

Catalyst system	Zr-RBS (wt.%)
Cp	0.60
<i>n</i> Bu	0.58
1:1 Cp: <i>n</i> Bu	0.39
1:3 Cp: <i>n</i> Bu	0.43
3:1 Cp: <i>n</i> Bu	0.53
1:1 <i>n</i> Bu:Cp	0.37
1:3 <i>n</i> Bu:Cp	0.47
3:1 <i>n</i> Bu:Cp	0.37

For example, 3:1 Cp:*n*Bu refers to catalysts systems prepared in a Cp₂ZrCl₂/(*n*BuCp)₂ZrCl₂ molar ratio in which Cp₂ZrCl₂ was initially immobilized onto silica, followed by (*n*BuCp)₂ZrCl₂ in a 3–1 molar ratio.

Table 1 shows the results of Zr content for different preparation procedures. The Zr contents are very similar, whatever the addition order, but for 3:1 Cp:*n*Bu and 3:1 *n*Bu:Cp the impregnation order affects the final result (0.53 vs. 0.37% total Zr). DRIFTS studies of the supported catalysts permit us to conclude that, even at the maximum amount of immobilization, there are remaining OH at the silica surface [11]. As shown in the spectrum **a** of Fig. 2, in the case of 1:1 *n*Bu:Cp system, there are still available OH groups (band at 3747 cm⁻¹). The bands at 2964–2936 cm⁻¹ correspond, respectively, to asymmetric ν(CH₃) and ν(CH₂), while those at 2880 and 2864 cm⁻¹, respectively, to symmetric ν(CH₃) and ν(CH₂) from butyl ligands. After addition of MAO in Al/Zr = 1000 ratio (spectrum **b**), the band attributed to isolated silanol disappeared and a large band centered at 2945 cm⁻¹ is observed due to presence of methyl groups from grafted MAO.

Table 2 presents data concerning catalyst activity and Mw of the polymers obtained with the homogeneous systems, simple and hybrid ones. In the case of simple catalysts, Cp activity is lower than that of Bu, although polymer Mw obtained with the former is higher. For hybrid catalysts, in

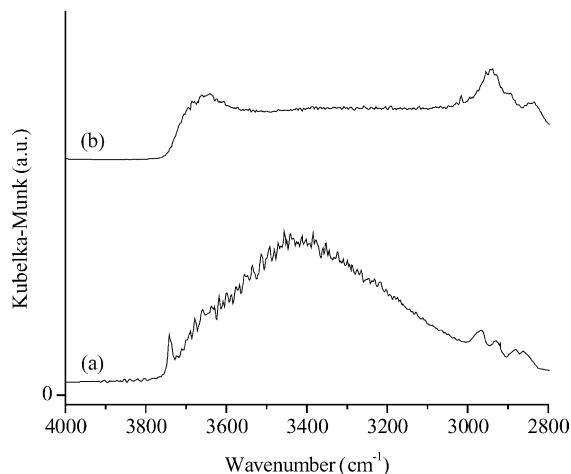


Fig. 2. DRIFTS spectra of (a) 1:1 *n*Bu:Cp catalyst system; (b) after addition of MAO [Al/Zr = 1000].

Table 2
Simple and hybrid homogenous catalysts

Catalyst system	Activity ($\times 10^3$ g Pol. (mmol Zr h) ⁻¹)	M_w ($\times 10^5$ g mol ⁻¹)	M_w/M_n	T_m (°C)
Cp	5.75	1.1	2.6	133
<i>n</i> Bu	7.34	0.7	2.5	133
1:1 Cp: <i>n</i> Bu	7.0	1.4	2.2	134
3:1 Cp: <i>n</i> Bu	4.9	1.0	2.0	134
1:3 Cp: <i>n</i> Bu	3.4	2.4	2.6	135

Activity and polymer characterization. [Al/Zr] = 1000; [Zr] = 1×10^{-5} M; solvent: toluene (300 cm³); $T = 60$ °C.

1:1 ratio catalyst activity roughly remains as the same as that observed in the case *n*Bu. Lower activity was observed for hybrid catalysts in 3:1 and 1:3 ratios. Mw increases in the following order: 3 : 1 < 1 : 1 < 1 : 3. Polydispersity of the polymer obtained with catalyst 1:3 is similar to that observed with simple systems (Table 3).

The supported catalysts show a complex behavior in terms of activity and molecular weight of the resulting polymer. Depending on the addition order and on the ratio between the zirconocenes, activities and molecular weights vary without an evident trend. Simple catalysts show similar activities. This fact implies that after the grafting step, Cp catalyst activity is reduced by a half, while *n*Bu to the third in comparison to those data observed for the homogeneous systems. Concerning 1:1 *n*Bu:Cp catalyst activity is 50% lower and Mw 20% higher than that observed in case of 1:1 Cp:*n*Bu. The 1:3 Cp:*n*Bu and 3:1 *n*Bu:Cp catalysts show the highest activities, almost twice of the simple catalysts, but molecular weight of resulting polymers produced by these catalysts is different (4.2 versus 3.3×10^5 Da). The 3:1 Cp:*n*Bu and 1:3 *n*Bu:Cp show similar activities but Mw data are totally different (3.1 versus 1.9×10^5 Da). The polyethylene Mw obtained with hybrid systems is between two and three times higher than obtained with simple systems.

Table 4 presents the structural parameter obtained from EXAFS measurements for 1:1 *n*Bu:Cp catalyst (2 adjustments considering distinct spheres of coordination) and 1:3 Cp:*n*Bu [12]. The EXAFS spectra of the two catalysts are totally different from that of Cp₂ZrCl₂ or ZrO₂. The analysis by Fourier Transformer shows two main peaks around

Table 3
Simple and hybrid supported catalysts

Catalyst system	Activity ($\times 10^3$ g Pol. (mmol Zr h) ⁻¹)	M_w ($\times 10^5$ g mol ⁻¹)	M_w/M_n	T_m (°C)
Cp	2.76	0.9	2.8	133
<i>n</i> Bu	2.60	1.5	2.4	133
1:1 Cp: <i>n</i> Bu	2.53	3.3	2.1	137
1:3 Cp: <i>n</i> Bu	5.45	4.2	2.0	135
3:1 Cp: <i>n</i> Bu	2.89	3.1	2.1	136
1:1 <i>n</i> Bu:Cp	1.69	3.8	2.1	135
1:3 <i>n</i> Bu:Cp	2.90	1.9	2.0	ND
3:1 <i>n</i> Bu:Cp	4.09	3.4	2.0	136

Activity and polymer characterization. [Al/Zr] = 1000; [Zr] = 1×10^{-5} M; solvent: toluene (300 cm³); $T = 60$ °C.

Table 4
Structural EXAFS parameters for selected systems

Catalyst system	Coordination number (<i>N</i>)	Distance <i>R</i> (Å)
1:1 <i>n</i> Bu:Cp		
Zr–O	1.1 ± 0.5	1.82 ± 0.02
Zr–C	1.8 ± 0.5	2.22 ± 0.02
1:1 <i>n</i> Bu:Cp		
Zr–O	1.4 ± 0.5	1.87 ± 0.02
Zr–Cl	0.5 ± 0.5	2.34 ± 0.02
Zr–Si	1.4 ± 0.5	3.29 ± 0.04
1:3 Cp: <i>n</i> Bu		
Zr–O	1.7 ± 0.5	1.9 ± 0.02
Zr–C	1.4 ± 0.5	2.3 ± 0.02
Zr–Si	1.6 ± 0.5	3.2 ± 0.04

Resolution 0.02 Å.

1.3 and 2.7 Å. Comparing Zr–C and Zr–O distances from both catalysts, 1:3 *n*Bu:Cp shows longer values than those found for 1:1 *n*Bu:Cp.

Table 5 presents data obtained in terms of relative energy in eV for the proposed reactions at the minimum distance found for Zr–O bond. These results allow us to establish that Cp₂ZrCl₂, due to the lack of sterical hindrance, is supported preferentially on the SiO₂AIS plane. In the case of (*n*BuCp)₂ZrCl₂ the energies permit us to think in a different distribution of this zirconocene and for Cp₂ZrCl₂ between these planes. From catalyst activity data, it is clear that using similar ratios (1:1), *n*Bu first generates a more active catalyst, being higher also the molecular weight.

Depending on the addition order and of the different ratios, AIS would present different concentrations/kinds of active sites, with higher or lower interaction between the zirconocenes. When *n*Bu is impregnated first, Cp can be grafted on SiO₂AIS at higher amounts. Cp shows high affinity for the AIS plane, whereas *n*Bu shows similar affinity for both planes. When Cp is first impregnated, it is located mainly on AIS plane, whereas *n*Bu is mainly fixed on GEM plane.

3.1. Mechanism of formation of active sites

MAO includes tricoordinated Al, capable to develop tetracoordination (terminal Al) and tetracoordinated Al generated by methyl addition/exchange. Tetracoordinated Al is a methyl donor, whereas tricoordinated Al is a methyl/electro/Cl acceptor [27]. Fig. 3 shows a possible mechanism of precursor of active site formation for these supported catalysts.

Table 5
Theoretical characterization results

SiO ₂	<i>n</i> Bu	<i>D</i> _{Zr–O}	Cp	<i>D</i> _{Zr–O}
AIS	–4.8	2.4	–10.9	1.45
GEM	–5.3	3.4	–5.6	2.80

Energy values in eV. Distances Zr–O at the energetic minimum-*n*Bu: (*n*BuCp)₂ZrCl₂; Cp: Cp₂ZrCl₂.

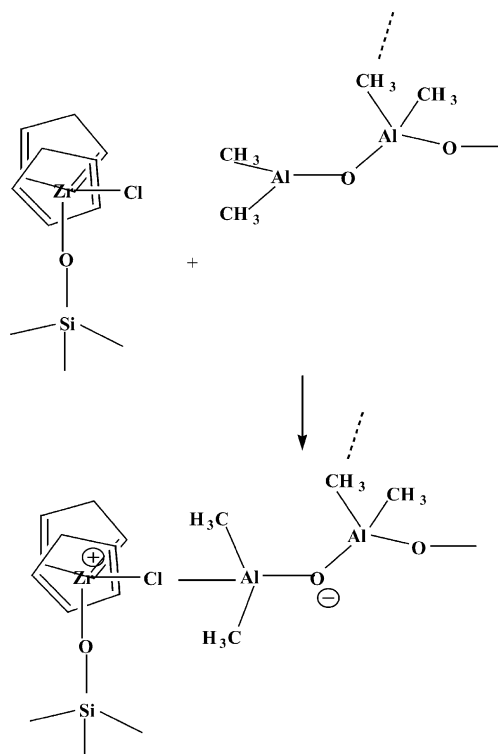


Fig. 3. First step of interaction of MAO with supported zirconocene.

Fig. 4 presents a possible mechanism of methylation of zirconocene and ion-pair formation on the surface. The ion-pair formation considers the coordination and insertion of ethylene by only one side of the supported zirconocene as the sole possibility. Fig. 5 shows a possible model of ethylene coordination. Comparing *n*Bu with Cp, the presence of butyl group impinges sterical hindrance to the ethylene approach in the *xy* plane, being lower the interaction when the approach takes place by the *zy* plane. In the case of Cp, there is no sterical hindrance for ethylene coordination in the *xy* plane.

3.2. General discussion

The supported catalyst 3:1 Cp:*n*Bu presents higher amount of grafted Zr and this fact can be assigned to the high affinity of Cp by the AIS plane of silica. In case of 3:1 *n*Bu:Cp, the steric effect introduced by butyl groups makes difficult the approach of Cp to the supported *n*Bu and therefore the amount of supported Zr is lower.

Analyzing the soluble systems, the decrease in activity can be assigned to bimolecular deactivation reactions and to the formation of binuclear cations of lower activity. It is known that active binuclear cations are present in the ethylene polymerization [22].

The presence of *n*Bu makes possible the formation of Cp-*n*Bu binuclear cations and increase the probability of formation of Zr1–CH₂–Zr2 bonds, with Zr1 and Zr2 belonging to different zirconocenes in homogeneous systems. Looking

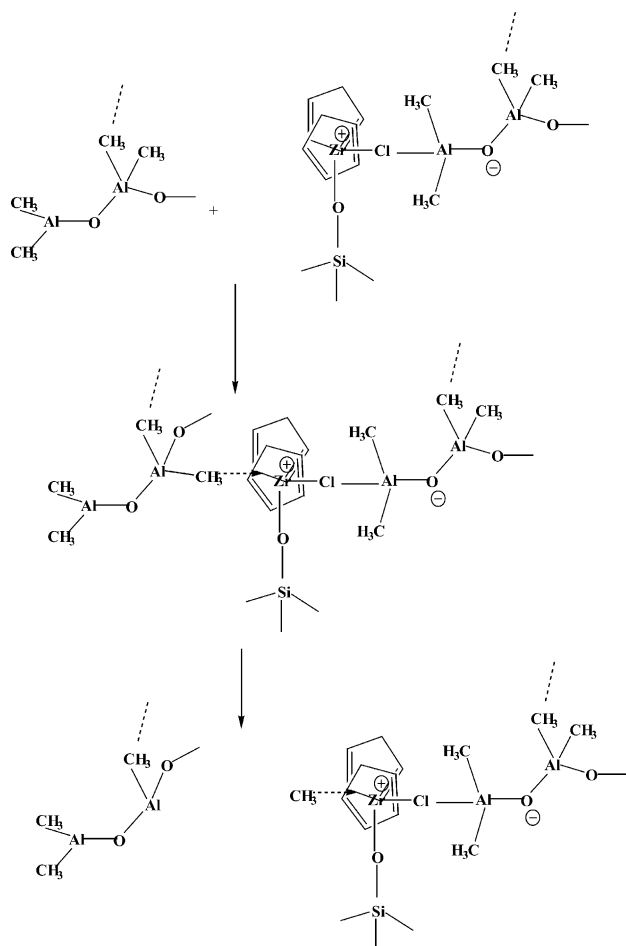


Fig. 4. Methylation of zirconocene and ion-pair formation.

at the supported systems, the decrease in the *n*Bu activity in respect to the soluble system can be assigned to the lower amount of active sites present on the AIS plane at the same concentration of supported zirconocene. However, in case of supported Cp, the relative number of species supported on the AIS silica plane is going to be higher, but the propagation constant is lower than in case of supported *n*Bu. The similar activities can be explained through a compensation effect between the active site number and the propagation constant. This kind of analysis is useful to investigate the increase of the activity when 1:3 Cp:*n*Bu or 3:1 *n*Bu:Cp are considered. Catalyst activity of 3:1 Cp:*n*Bu is similar to that of the simple systems, but molecular weights of the resulting polymers are three times higher than those obtained with the homogeneous systems.

The molecular weights of polyethylene obtained with 1:1 Cp:*n*Bu, 3:1 Cp:*n*Bu and 3:1 *n*Bu:Cp are similar. This fact can be related to a different number/distribution of active sites, although being the same kind of active sites. In the case of 3:1 Cp:*n*Bu the molecular weight increases significantly in respect to the simple catalysts, whereas with 1:3 *n*Bu:Cp the molecular weight of polyethylene is in the order of the simple catalysts. Distribution of sites on the SiO₂AIS

with supported *n*Bu working independently from Cp can be related to the maximum activity and molecular weight, whereas the interaction *n*Bu:Cp with *n*Bu as Cp modifier can explain the decrease of the molecular weight because of the decreased strength of the Zr–C bond. Inactive sites concentration is also different depending on the addition order and on the different zirconocenes ratio. In case of 1:3 Cp:*n*Bu the high activity can be related to the consumption of geminal OH by Cp and the higher amount of active sites from supported *n*Bu on the SiO₂AIS plane. This mechanism is proposed following the concepts reported in reference [26].

3.2.1. Interaction between supported zirconocenes

A possibility to take into account is the interaction of the different zirconocenes on the surface. If we consider that Cp₂ZrCl₂ can modify *n*BuCp₂ZrCl₂, the resulting sites would have different properties than those generated by immobilizing independently each zirconocene on the surface. Fig. 6 shows a model of interaction of this binuclear active site with MAO. Even being Cp only a dispersor of *n*Bu, it is evident that this effect is important particularly on the molecular weight. The possibility of interactions in *n*Bu:Cp giving rise to active Cp modified by *n*Bu or active *n*Bu modified by Cp cannot be ruled out. These sites would have activities and termination constants for the growing polyethylene chain different from that of the isolated supported Cp or *n*Bu.

Concerning the homogeneous systems, we consider that *n*Bu has higher activity because almost no binuclear sites are formed, whereas in case of Cp, there is no steric hindrance to the Cp₂ formation. Therefore, Tables 6 and 7 resume this information. In case of the supported catalysts we can see that Cp and *n*Bu have similar activities, but molecular weight is different for the polymer. If we consider that *n*Bu presents a higher propagation constant we can understand the results for the supported catalyst.

In the case of 1:1 Cp:*n*Bu, Cp is located on AIS (following the EHMO results) and the structures are different from those in the case of the homogeneous system and this is clear from the molecular weight analysis. Cp:*n*Bu sites are also present. Number of active sites must be different (lower) but propagation constant could be higher, changing also the termination reactions. The catalyst addition order changes the number and distribution of sites. When 1:1 *n*Bu:Cp is analyzed, activity is higher, even in comparison to that of the

Table 6
Active sites present in homogeneous systems

Homogeneous				
Cp	<i>n</i> Bu	1:1 Cp: <i>n</i> Bu	3:1 Cp: <i>n</i> Bu	1:3 Cp: <i>n</i> Bu
Cp	<i>n</i> Bu	Cp	Cp	Cp
Cp ₂	<i>n</i> Bu ₂	Cp ₂	Cp ₂	Cp ₂
		Cp: <i>n</i> Bu	Cp: <i>n</i> Bu	Cp: <i>n</i> Bu
		<i>n</i> Bu	<i>n</i> Bu	<i>n</i> Bu

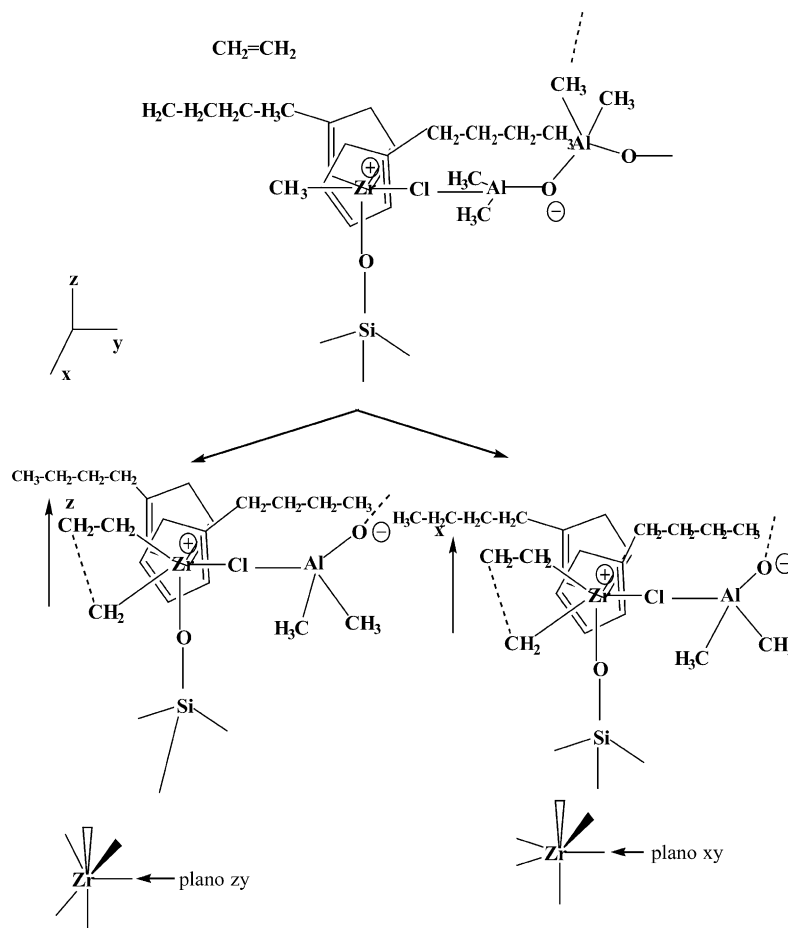


Fig. 5. Model of ethylene coordination.

soluble catalyst. If *n*Bu is located widespread on the surface, but the most active sites are placed in SiO₂AlSi, Cp addition generates especially *n*Bu:Cp sites, but probably not Cp₂. Therefore we have *n*Bu and *n*Bu:Cp species, more active than Cp, Cp₂ and *n*Bu:Cp species. If we consider that

the activity of the species changes in the order *n*Bu > Cp > Cp₂ > *n*Bu : Cp, for homogeneous system and this order changes when Cp and *n*Bu are supported we can explain all the results. Molecular weight is lower for *n*Bu in this case. Specifically, the activity order in the heterogeneous catalyst would be *n*Bu : Cp > *n*Bu = Cp > Cp₂. In the case of *n*Bu versus Cp, we do not know if we have similar active sites number with similar propagation constants (but lower growing chain termination constant) or lower/higher amount of active sites with higher/lower propagation constant and lower growing chain termination constants. Molecular weight of polymer produced by supported *n*Bu is higher than Cp in this case, and therefore active sites have different ratio propagation to termination constants. The effect of the support as ligand is very important to change this order. Both electronic and geometric factors contribute to achieve this activity order. For these reasons, changes must surely arise when *n*Bu is supported, related to the presence of the support as a ligand, combined with the effect of the butyl groups. In case of 1:3 Cp:*n*Bu and 3:1 *n*Bu:Cp, activities are similar. We can think that *n*Bu is in an isolated form at high concentration in this case, especially in the first case, when Cp is a dispersant species for *n*Bu on the surface and mainly the isolated AIS plane is covered by Cp. In the

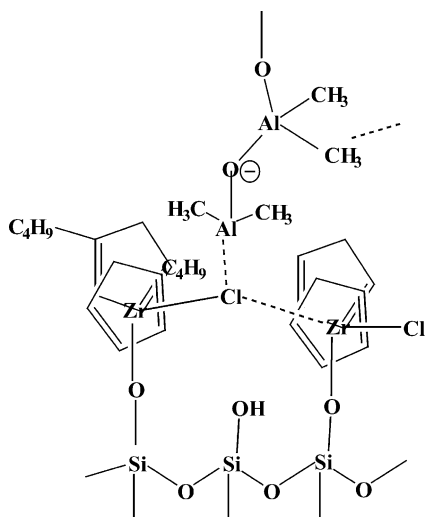
Fig. 6. Model of a binuclear active site in *n*Bu:Cp-*n*Bu upon methylation.

Table 7
Active sites present in heterogeneous systems

Cp	<i>n</i> Bu	1:1 Cp: <i>n</i> Bu	1:3 Cp: <i>n</i> Bu	3:1 Cp: <i>n</i> Bu	1:1 <i>n</i> Bu:Cp	1:3 <i>n</i> Bu:Cp	3:1 <i>n</i> Bu:Cp
Cp	<i>n</i> Bu	CpAIS <i>n</i> BuAIS Cp: <i>n</i> Bu	CpAIS <i>n</i> BuAIS Cp: <i>n</i> Bu	CpAIS <i>n</i> BuAIS Cp: <i>n</i> Bu	CpAIS <i>n</i> BuAIS Cp: <i>n</i> Bu	CpAIS <i>n</i> BuAIS Cp: <i>n</i> Bu	CpAIS <i>n</i> BuAIS Cp: <i>n</i> Bu
Cp2		Cp2	Cp2	Cp2		Cp2	

second case, *n*Bu is distributed on the surface and the relative amount of *n*Bu must be higher than in case 1. But the difference is the relative amount of Cp isolated active sites and *n*Bu:Cp sites. Therefore molecular weight is different. If *n*Bu:Cp sites have high propagation constant when they are supported, distribution of Cp and *n*Bu isolated besides *n*Bu:Cp must be considered. It is worth noting that the activity is near the Cp homogeneous activity. When 3:1 Cp:*n*Bu systems are analyzed, the potential sites at the AIS plane are covered first by Cp and Cp2 and consequently activity is lower. However, *n*Bu:Cp sites are present and this is clear from the molecular weight of the produced polymers. It is worth noting that the activity of 3:1 Cp:*n*Bu is almost the same as supported Cp and *n*Bu but molecular weight is two or three times higher. Compensation effects can explain the activity but the molecular weight allow us to conclude that *n*Bu:Cp, *n*Bu and Cp sites distribution and amount are different in these cases. Table 7 shows that in case of 1:1 or 3:1 *n*Bu:Cp probability of Cp2 formation on the surface is lower, considering the EHMO results.

3.2.2. Molecular weight distribution of polyethylenes

From Table 2, the Mw/Mn values for homogeneous catalyts Cp and *n*Bu are 2.6 and 2.5, whereas in case of supported catalysts, the polydispersities are 2.8 and 2.4. In the first case we have homogeneous sites, without silica present, whereas in the second one we have heterogeneous sites involving silica. The idea of a *single* site producing narrow Mw/Mn has been seriously criticised by Prof. James C.W. Chien and his group some time ago [28,29]. They performed a complete characterization of several soluble and supported metallocene//MAO systems. They proposed that different sites with different propagation and transfer constants but with similar ratio propagation to transfer constants can produce narrow polymer distributions as obtained with metallocenes//MAO systems. Difference in sites structures are evident in the yield in grams for a specific catalyst, that are different for different metallocenes and in the microstructure of the produced polymer. This fact can be clearly demonstrated when propylene is polymerized using metallocene/MAO. This fact is clear in our manuscript from Tables 2 and 3 for Cp and *n*Bu separately and comparing the hybrid systems. The criterion for single site cannot be therefore Mw/Mn = 1.5–2. We explain our results because Cp and *n*Bu have different propagation constants and termination constants, being different zirconocenes, in ethylene polymerization but ratio of propagation to

termination constants are similar. Moreover, narrow MWD polyolefins do not have the desired balance of rheological and physical–mechanical properties. Increase of MWD can be achieved by using two or more metallocenes with different central atom or completely different structure (for instance hafnocene and zirconocene, nonbridged and bridged). Trimodal or even broader MWD is possible by this approach. Judicious mixing of metallocenes having C_{2v} and C₂ symmetries can produce an in situ blend of high MW atactic PP and moderate MW iPP which will possess properties of TPE-PP. In our case probably depending on temperature, MAO concentration and zirconocene concentration, Cp and *n*Bu separately present in the reaction media different active sites whose ratio changes but all these different active sites have similar ratios from termination to propagation constant. We can appreciate the differences in activity (related to propagation constant) and molecular weight (related to termination constant) for each catalyst, soluble or supported presented in Tables 2 and 3.

Acknowledgements

M.L. Ferreira acknowledges CONICET by the financial support. Dos Santos and his group are thankful for CNPq by the financial support.

References

- [1] M. Jezequel, V. Dufaud, M.J.R. Garcia, F.C. Hermosilla, U. Neugebauer, G.P. Niccolai, F. Lefebvre, F. Bayard, J. Corker, S. Fiddy, J. Evans, J.P. Broyer, J. Malinge, J.M. Basset, *J. Am. Chem. Soc.* 123 (2001) 3520.
- [2] J. Tian, S. Wang, Y. Feng, J. Li, S. Collins, *J. Mol. Catal. A: Chem.* 144 (1999) 137.
- [3] G.G. Hlatky, *Chem. Rev.* 100 (2000) 1347.
- [4] J.D. Kim, J.B.P. Soares, G.L. Rempel, *Macromol. Rapid Commun.* 19 (1998) 197.
- [5] L. D'Agnillo, J.B.P. Soares, A. Penlidis, *J. Polym. Sci. Part A: Polym. Chem.* 36 (1998) 831.
- [6] T.K. Han, H.K. Choi, D. W. Jeung, Y.S. Ko, S.I. Woo, *Macromol. Chem. Phys.* 196 (1995) 2637.
- [7] J.S. Chung, H.S. Cho, Y.G. Ko, W.Y. Lee, *J. Mol. Catal. A: Chem.* 144 (1999) 61.
- [8] H.S. Cho, Y.H. Choi, W.Y. Lee, *Catal. Today* 63 (2000) 523.
- [9] H.S. Cho, J.S. Chung, W.Y. Lee, *J. Mol. Catal. A: Chem.* 159 (2000) 203–213.
- [10] M.M.deC. Forte, F.V. da Cunha, J.H.Z. dos Santos, *J. Mol. Catal. A: Chem.* 175 (2001) 91.
- [11] F. Silveira, S.R. Loureiro, G.B. Galland, F.C. Stedile, J.H.Z. dos Santos, T. Teranishi, *J. Mol. Catal. A: Chem.* 206 (2003) 389.

- [12] F. Silveira, S.R. Loureiro, G.P. Pires, M. do C. Alves, F.C. Stedile, J.H.Z. dos Santos, K.M. Bichinho, T. Teranishi, X-Ray Spectrometer, submitted for publication.
- [13] J.H.Z. dos Santos, P.P. Greco, F.C. Stedile, J. Dupont, J. Mol. Catal. A: Chem. 154 (2000) 103–113.
- [14] M.L. Ferreira, P.P. Greco, J.H.Z. dos Santos, D.E. Damiani, J. Mol. Catal. A: Chem. 172 (2001) 97.
- [15] F.C. Stedile, J.H.Z. dos Santos, Nucl. Instrum. Meth. B 1259 (1998) 136.
- [16] F.C. Stedile, J.H.Z. dos Santos, Phys. Stat. Sol. (a) 173 (1999) 123.
- [17] T. Ressler, J. Phys. IV 7 (1997) 269.
- [18] J.J. Rehr, J.M. De Leon, S.I. Zabinsky, R.C. Albers, J. Am. Chem. Soc. 113 (1991) 5135.
- [19] R. Hoffmann, Solids and Surfaces: A Chemist's View of Bonding in Extended Structures, Cuch, New York, 1988 and references therein.
- [20] A. Anderson, R. Hoffmann, J. Chem. Phys. 60 (1974) 4271.
- [21] J. Kamber, L. Forrs, G. Calzaferri, J. Phys. Chem. 93 (1989) 5366.
- [22] T. Haselwander, S. Beck, H.H. Brintzinger, in: G. Fink, R. Mülhaupt, H.H. Brintzinger (Eds.), Ziegler Catalysts, Springer, Germany, 1995, p. 181.
- [23] J.L. Atwood, W.E. Hunter, D.C. Hrcir, E. Samuel, H. Alt, M. Rausch, Inorg. Chem. 14 (1975) 1757.
- [24] F. Wochner, L. Zsolnai, G. Huttner, H.H. Brintzinger, J. Organomet. Chem. 288 (1985) 69.
- [25] F.R.W.P. Wild, M. Wasiucioneck, G. Huttner, H.H. Brintzinger, J. Organomet. Chem. 288 (1985) 63.
- [26] M.L. Ferreira, Macromol. Theory Simulat. 11 (2002) 250.
- [27] M.L. Ferreira, P.G. Belelli, A. Juan, D.E. Damiani, Macromol. Chem. Phys. 201 (2000) 1334.
- [28] J.C.W Chien, in: G. Fink, R. Mülhaupt, H.H. Brintzinger (Eds.), Ziegler Catalysts, Springer, Verlag, Germany, 1995, p. 199.
- [29] J.C.W. Chien, R.J. Sugimoto, Polym. Sci. Part A 29 (1991) 4591.